



Ga-vacancy induced room temperature ferromagnetism observed in N-irradiated GaN films



Juping Xu^a, Qiang Li^{a,b}, Wenshuai Zhang^a, Jiandang Liu^a, Huaijiang Du^a, Bangjiao Ye^{a,*}

^a State Key Laboratory of Particle Detection and Electronics, University of Science and Technology of China, Hefei 230026, China

^b China Spallation Neutron Source, Institute of High Energy Physics, Chinese Academy of Sciences, Dongguan 523803, China

ARTICLE INFO

Article history:

Received 26 August 2014

In final form 19 October 2014

Available online 24 October 2014

ABSTRACT

GaN films prepared on sapphire substrates with thickness of 30 μm, were implanted by nitrogen ions with energy of 80 keV at doses of $5 \times 10^{16} \text{ cm}^{-2}$ and $2 \times 10^{17} \text{ cm}^{-2}$, respectively. An obvious ferromagnetic loop was obtained in the higher dose irradiated GaN film at room temperature, indicating magnetic defects were induced into this film. After irradiation, the films contained lots of Ga vacancies were investigated by slow positron annihilation spectroscopy. With first-principle calculations, we demonstrated that Ga vacancies could lead to an enhancement of magnetic moment for 3 μB in GaN crystal and form ferromagnetic coupling at room temperature between two close range Ga vacancies.

© 2014 Elsevier B.V. All rights reserved.

1. Introduction

Dilute magnetic semiconductors (DMSs) have been attracting much attention in recent years due to their feasibility of fabricating spintronic devices. Compared with the traditional transition-metal elements doping [1–4], defect-induced magnetism (DIM) can reach an un-expected high temperature ferromagnetism, which is so called d0 ferromagnetism [5]. Since the first discovery of DIM in HfO₂ films [6], this unique property is also demonstrated by theories and experiments in plenty of other semiconductors such as TiO₂, ZnO, MgO, etc. [7–9], while the origin of the magnetic order still under challenges since the otherwise non-magnetism was observed in these defective materials. Moreover, GaN as one of the most important III–V group semiconductors also has been investigated in DMSs field extensively due to its potential applications such as blue or green optoelectronics, nuclear battery and detectors [10–12]. Nonetheless, the origin and mechanism of DIM in GaN-based DMSs also have not reached a unanimous opinion so far. For instance, some experimental researchers observe room temperature ferromagnetism (RTFM) in GaN nanoparticles or films and attribute it to Ga-related vacancies [13–15]. However, ferromagnetism cannot reach to room temperature when the vacancy density is lower than 10^{21} cm^{-3} , which has been predicted by theoretical calculations [16]. And some others owe the room temperature ferromagnetism finding in semiconductors to

the impurities in the samples which were doped unintentionally or by pollution [17].

Actually, despite the huge amount of reports on transition-metal doped DMSs, there are few of works focus their attention on defect magnetism in GaN crystal. Impurities also should be carefully characterized with the best available methods into this research field, which has been clearly presented in recent studies [18,19]. Therefore, more efficient studies should be done to show some deep insight in this interesting issue. In this work, we choose method of ion implantation to import N particles, which is an effective way to avoid other impurity elements and will induce lattice vacancies only [20]. The magnetism behavior of irradiated samples is measured by vibrating sample magnetometer. The irradiation-induced damage and vacancy-related defect are characterized by Raman spectra and positron annihilation spectroscopy, respectively. Furthermore, the first-principles calculations based on density functional theory are also employed to study the relevance of defect-structure and magnetic properties in hexagonal GaN crystal, and to verify the results of experiments.

2. Experiment

The n-type GaN films with thickness of 30 μm are grown on sapphire substrates by hydride vapor phase epitaxy, which is obtained commercially from Kejing Materials Company, Hefei. The sample is cut into three parts with the size of 6 mm × 8 mm, and one of them is maintained as a reference.

As well known that the magnetic impurities such as Fe, Co, Ni, etc. might influence the results, so that make some researchers

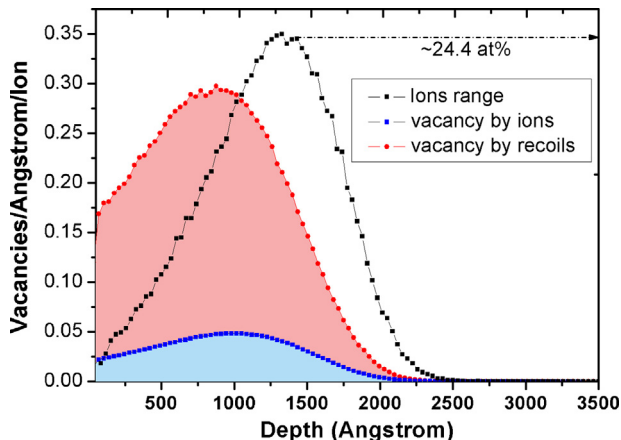
* Corresponding author.

E-mail address: bjye@ustc.edu.cn (B. Ye).

Table 1

Results of LA-ICPMS analysis.

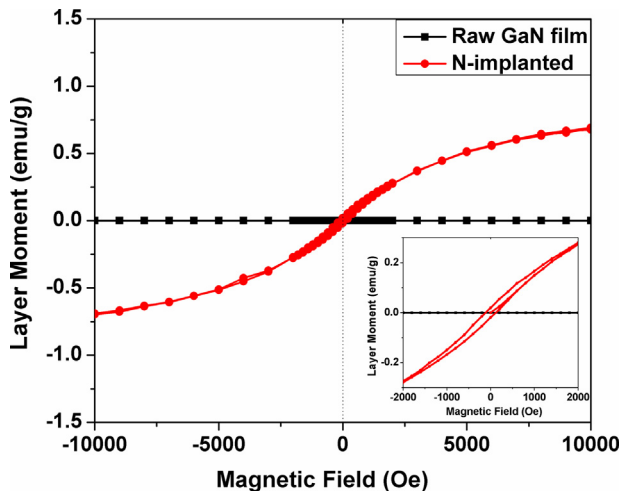
	Fe	Co	Ni	Cr	Mn
Concentrations (ppm)	45	–	2	10	3
Moment (emu/g $\times 10^{-4}$)	99	–	1.1	2.2	3.6

**Figure 1.** The distribution of implanted N ion for $2 \times 10^{17} \text{ cm}^{-2}$ dose and damage caused by implanted and recoiling ions estimated by SRIM.

doubt the magnetism observed in DIMs. In order to clarify this problem, we use Laser Ablation Inductively Coupled Plasma Mass Spectroscopy (LA-ICPMS) to detect ferromagnetic impurities in virgin sample [21], the main results are shown in **Table 1**. We can find that the total content of magnetic impurities is about 60 ppm. Based on the average saturation moment of those elements suggested in references, the total magnetism moment in the whole wafer is about 0.01 emu/g.

N-ions irradiation is carried out using ions implanter at college of Nuclear Science and Technology, Beijing Normal University. The N ions are accelerated to 80 keV and injected into two GaN films with total influence of $5 \times 10^{16} \text{ cm}^{-2}$ and $2 \times 10^{17} \text{ cm}^{-2}$, respectively. The injection process maintain at approximately room temperature and no immediately annealing after implantation. The average implantation length ways depth and inject-induced defects are simulated by Stopping and Ranges of Ions in Matter (SRIM) program, as shown in **Figure 1**. The implantation layer is estimated about 150 nm range of 50–200 nm and the implanted peak of atomic concentrations is about 7.5 at.% and 24.4 at.% for $5 \times 10^{16} \text{ cm}^{-2}$ and $2 \times 10^{17} \text{ cm}^{-2}$ doses, respectively. The red and blue regions represent the content of vacancy type defect made by implanted and recoiled ions. This simulation result indicates that track direction of N ions is strongly changed by target lattice scattering, causing vacancy-related damage during recoiling stronger than that during implantation. The vacancies distribute from surface into the implanted region, and the profile is different from that of N ions.

Vibrating samples magnetometry (VSM) with an accuracy of 10^{-7} emu is used to determine the magnetic properties. The defects information can be observed by Raman and slow position annihilation spectra. Raman scattering is measured with Ar⁺ 514 nm laser lines as an excitation light source, ranging from 100 cm^{-1} to 800 cm^{-1} . In addition, mono-energetic slow positron beam generated from ²²Na radioactive source with the energy varied from 0.25 to 20 keV is used as lattice probe in our positron annihilation spectroscopy. Positron annihilation techniques considered as a unique probe nondestructive have been used widely in the research of materials [22]. Doppler broadening of annihilation radiation is measured by an HPGe Detector with energy resolution of 0.2%.

**Figure 2.** The room temperature field-dependent magnetization curves of unimplanted GaN film and N-implanted film with higher dose of $2 \times 10^{17} \text{ cm}^{-2}$.

Positrons will easily be trapped in vacancy-typed defects and then annihilate with valence electrons at atomic outers, which results in a narrowing of the 511 keV annihilation peak compared to bulk annihilation. The ratio of counts in the central region to the total number of counts in the 511 keV peak is defined as 'S parameter'. Thus, positrons trapped in vacancy defects will result in an increase in S, which is proved strongly relevant to the Ga-vacancy related defects in GaN sample [23,24].

3. Results and discussion

The magnetic property of samples is determined at 300 K, as shown in **Figure 2**. The raw GaN film shows a rigorous diamagnetism by the M-H curves, also the implanted sample with lower dose of N-ions shows diamagnetic property, no obvious RTFM signal is detected in the films. While continue to increase the implantation dose to $2 \times 10^{17} \text{ cm}^{-2}$, the M-H curve shows distinct S-shaped indicating the magnetic behavior change occurs in this sample. The inset definitely shows that the room temperature ferromagnetism is introduced in GaN film after N implantation with certain dose. This curve is treated to subtract diamagnetic background signals. The saturation moment (M_S) is estimated about 0.7 emu/g, and the coercive force (H_C) is about 120 Oe, which is greatly (about 70 times) larger than that caused by impurities. Consider that the N-implantation cannot introduce any other foreign elements in the film, we infer that the observed RTFM will mostly relevance to inject-induced lattice-defects by N ions. We introduce Raman spectra and positron annihilation spectroscopy to detect the sample structure after implantation, and the results are shown in **Figure 3**.

Figure 3a shows the optical properties of as-implanted and N-implanted GaN films with Raman spectrum. For wurtzite structure, the Raman active phonon modes expected from group theory are $A_1 + E_1 + 2E_2$, where A_1 and E_1 split into longitudinal optical (LO) and transverse optical (TO) [25]. In addition to the substrate phonon modes of 418 cm^{-1} , the expected first order permissible phonon modes according to the selection rule, which is located at 144 cm^{-1} [$E_2^{(\text{low})}$], 570 cm^{-1} [$E_2^{(\text{high})}$], 734 cm^{-1} [$A_1^{(\text{LO})}$], can be found in the raw GaN film spectra. The intensity of 570 cm^{-1} [$E_2^{(\text{high})}$], and 734 cm^{-1} [$A_1^{(\text{LO})}$] peaks sharply decrease after N implantation along increasing dose, which most likely related to the lattice disorder due to ion implantation. Compared with pure GaN film, new broad peak around the frequencies of 300 cm^{-1} , 418 cm^{-1} and 669 cm^{-1} are observed in the N-implanted sample.

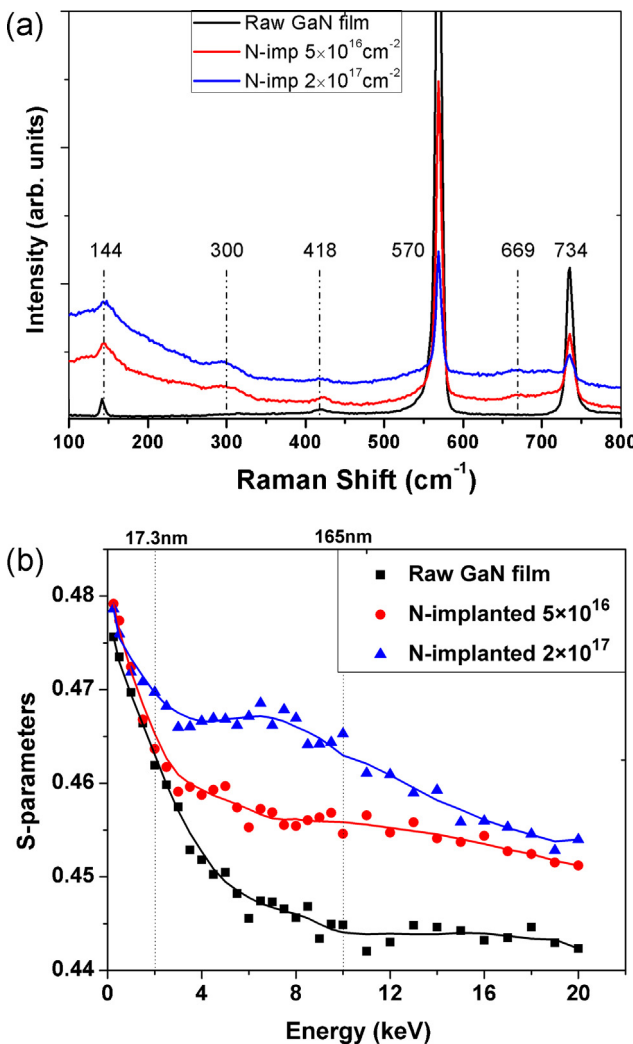


Figure 3. (a) Raman spectra and (b) the S parameter as a function of incident positron energy for as-implanted and N-implanted samples.

The mode of 300 cm^{-1} is caused by lattice disorder also. Moreover, the vibration modes at 418 cm^{-1} and 669 cm^{-1} are considered as defect-induced modes, the previous literatures ascribed those two peaks to N- and/or Ga-vacancy [26]. However, they are too weak to be recognized by Raman spectra in our implanted GaN samples.

For further demonstrating the structure changes of these irradiated samples, Doppler broadening annihilation spectrum measured by slow positron spectroscopy is shown in Figure 3b. Figure 3b displays the S parameter as a function of incident positron energy for as-implanted and N-implanted samples. Based on VEPFIT fitting [27], the curves can be divided into three layers, they are surface, irradiated region and Al_2O_3 substrate. The surface layer usually exhibits high S -parameters due to the formation of positronium atoms at material surface [19]. As shown in the top axes of Figure 3b, the irradiated layer is range from 17 nm to 165 nm, which is corresponding to positron energy range of 2–10 keV. The region and thickness of this layer is good agreement with the simulation result of SRIM mentioned above. The S -curves for N-implanted films is obviously larger than that of raw GaN film and the S -parameters increase with the dose increasing of N-ions. It means that the N-implantation induce a lot of Ga-vacancies in GaN samples, also the vacancy contain is much larger in higher dose implanted sample than others. As a consequence, the RTFM is only obtained in this higher dose implanted films. As mentioned above, the RTFM cannot be attributed to the magnetic impurities since the content of

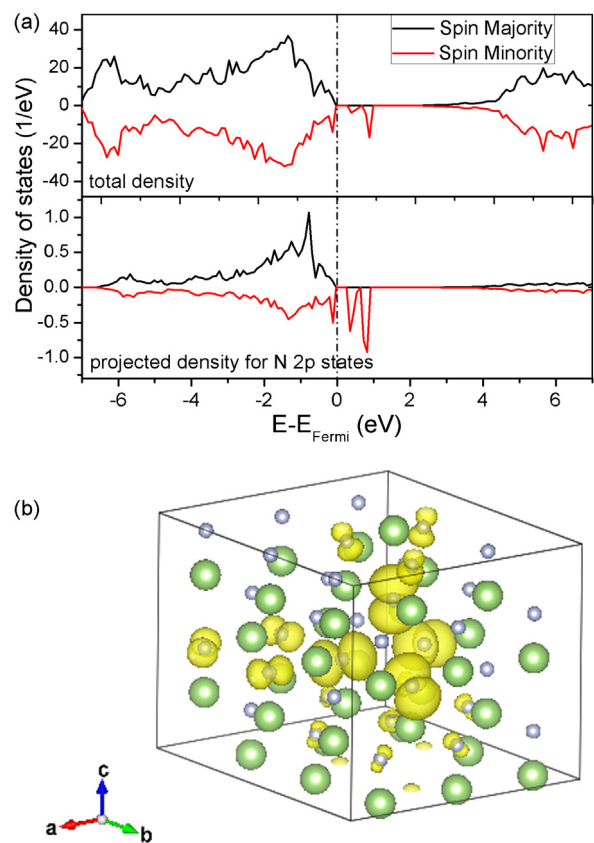


Figure 4. (a) The density of electronic states of $\text{Ga}_{35}\text{V}_{\text{Ga}}\text{N}_{36}$ supercell (up) and the N atoms around the Ga-vacancy (down); (b) the isosurface charge density plots ($\rho = 0.0135\text{ e}/\text{\AA}^3$) of the spin-minority states of $\text{Ga}_{35}\text{V}_{\text{Ga}}\text{N}_{36}$ supercell.

those elements are very small and no any ferromagnetic behavior is observed in raw GaN films. On the other hand, there are no definite N-related vacancies are detected in our Raman experiment. Thus, we believe that the positron annihilation spectroscopy shows experimental evidence of exclusively Ga vacancy can induce RTFM in GaN materials, which is in good agreement with the conclusion drawn by Roul et al. [15].

In order to give further insight in Ga-vacancy induced RTFM in GaN material, we make use of the Vienna Ab-initio Simulation Package [28] based on density-functional theory within generalized gradient approximation method to calculate the magnetic property of Ga vacancy in $\text{Ga}_{35}\text{V}_{\text{Ga}}\text{N}_{36}$ supercell (wurtzite structure). The Perdew–Burke–Ernzerhof [29] exchange-correlation function is used to produce the density of states and the irreducible Brillouin zone for the supercell uses Monkhorst–Pack method to generate $4 \times 4 \times 4 k$ -points. The chosen cutoff energy is 400 keV during structure optimization and static computation process.

As shown in Figure 4a, the total density of electronic states of $\text{Ga}_{35}\text{V}_{\text{Ga}}\text{N}_{36}$ displays an electronic spin splitting state between the valence band and conduction band, while this splitting impurity band is not observed in perfect $\text{Ga}_{36}\text{N}_{36}$ wurtzite structure. The calculated band gap is about 2.48 eV, which is smaller than experimental value. In this structure with a Ga atom taken away, the spin-polarized states are generated near the top of valence band and whole supercell show local magnetic moments with about $3\text{ }\mu\text{B}$ per Ga-vacancy, which is in good agreement with the previous reports [16,30]. The projected density of states clearly indicates that the magnetic impurity band is mainly contributed by N 2p orbit nearby this Ga-vacancy. From the isosurface charge density plots of the spin-minority states as shown in Figure 4b, we observe the polarization charge mainly located around Ga-vacancy, and more

Table 2

Magnetic coupling of two Ga vacancies for different distances.

D Å	ΔE meV	J_0
5.29	171.59	19.07
5.60	97.86	10.87
6.17	28.55	3.17
6.47	-52.63	-5.85
9.70	-60.59	-6.73

close of N atoms to the Ga vacancy center, the stronger of polarization degree of the N 2p orbit.

We calculate the magnetic coupling of two Ga vacancies about $\text{Ga}_{34}(\text{V}_{\text{Ga}})_2\text{N}_{36}$ supercell with different distance, and the results are shown in Table 2. The energy difference between ferromagnetic and antiferromagnetic phase is defined as $\Delta E = E_{\text{AFM}} - E_{\text{FM}} = 4J_0S^2$, according to Heisenberg model [31], where J_0 is the nearest-neighbor exchange parameter and S is 3/2, to evaluate the ground state stability and magnetic interaction. We discover that the ΔE increase sharply with distance reduce of two Ga vacancies, and induce in crucial transformation of $V_{\text{Ga}}-V_{\text{Ga}}$ coupling from antiferromagnetism to ferromagnetism. When the $V_{\text{Ga}}-V_{\text{Ga}}$ distance is larger than 6.47 Å, the magnetic coupling between them is tend to form antiferromagnetic interaction, which can be described with virtual electron exchange mechanism, as suggested in previous report [30]. However, the ferromagnetic interaction between the closed Ga-vacancies is out of the reach of this mechanism. The coupling of closed Ga-vacancy give a higher J_0 value reach to about 19.07, indicating that the ferromagnetism can exist stably in GaN material under room temperature. This result is in good conformity with our experimental reference discussed above as well as previous report [30]. We confirm that the Ga vacancies can induce room temperature ferromagnetism in GaN film, and interpret the phenomenon that the ferromagnetic behavior is strongly depended on the density of defects, which may be depicted by a bound magnetic polaron mechanism [32,33]. It is worthy to note that we also calculate the supercell contained one N-vacancy. The results indicate that system with one N vacancy can display magnetic moment about 0.7 μB , while further calculation confirm that the moments are non-local, thus no macromagnetic coupling occurring among N vacancies.

In conclusion, we prepare GaN films and implant them with N ions under the fluence of $5 \times 10^{16} \text{ cm}^{-2}$ and $2 \times 10^{17} \text{ cm}^{-2}$, respectively. The Raman spectrum and positron annihilation spectroscopy confirm that the RTFM observed in irradiated film is attributed to Ga-vacancy-related defects. The density-functional theory calculation confirms the result of experiments. Moreover, we observe that the strength of ferromagnetic coupling of Ga vacancies increase

with the distance decrease of them, and lead to the transform from antiferromagnetism to ferromagnetism.

Acknowledgements

We gratefully acknowledge Professor Zhenhui Hou in assistance with LA-ICPMS measurements. This work is supported by the National Natural Science Foundation of China (Grant Nos. 11175171 and 11105139).

References

- [1] H.H. Nguyen, J. Sakai, W. Prellier, A. Hassini, A. Ruyter, G. Francois, Phys. Rev. B 70 (2004) 195204.
- [2] N.A. Spaldin, Phys. Rev. B 69 (2004) 125201.
- [3] Y.W. Heo, et al., Appl. Phys. Lett. 84 (2004) 2292.
- [4] K.A. Griffin, A.B. Palkhomov, C.M. Wang, S.M. Heald, K.M. Krishnan, Phys. Rev. Lett. 94 (2005) 157204.
- [5] J.M.D. Coey, Solid State Sci. 7 (2005) 660–667.
- [6] M. Venkatesan, C.B. Fitzgerald, J.M.D. Coey, Nature 430 (2004) 630.
- [7] S.D. Yoon, et al., J. Phys.: Condens. Matter 18L (2006) 355–361.
- [8] N.H. Hong, J. Sakai, N. Poirot, V. Brize, Phys. Rev. B 73 (2006) 132404.
- [9] M. Kapilashrami, J. Xu, K.V. Rao, L. Belova, E. Carlegrim, M. Fahlman, J. Phys.: Condens. Matter 22 (2010) 345004.
- [10] F.A. Ponce, D.P. Bour, Nature 386 (1997) 351.
- [11] R. Dahal, J. Li, K. Aryal, J.Y. Lin, H.X. Jiang, Appl. Phys. Lett. 97 (2010) 073115.
- [12] M. Asif Khan, J.N. Kuznia, D.T. Olson, J.M. Van Hove, M. Blasingame, Appl. Phys. Lett. 60 (1992) 2917.
- [13] C. Madhu, A. Sundaresan, C.N.R. Rao, Phys. Rev. B 77 (2008) 201306R.
- [14] H. Ren, et al., Appl. Phys. A (2013), <http://dx.doi.org/10.1007/s00339-013-8065-9>.
- [15] B. Roul, et al., Appl. Phys. Lett. 99 (2011) 162512.
- [16] X. Wang, M. Zhao, T. He, Z. Wang, X. Liu, Appl. Phys. Lett. 102 (2013) 062411.
- [17] L. Yu, Z. Wang, M. Guo, D. Liu, Y. Dai, B. Huang, Chem. Phys. Lett. 487 (2010) 251–255.
- [18] M. Khalid, A. Setzer, M. Ziese, P. Esquinazi, D. Spemann, A. Pöppel, E. Goering, Phys. Rev. B 81 (2010) 214414.
- [19] Q. Li, et al., Chem. Phys. Lett. 556 (2013) 237–241.
- [20] Shengqiang Zhou Nuclear Instruments, Methods Phys. Res. B 326 (2012) 55.
- [21] C.J. Pickford, R.M. Brown, Spectrochim. Acta B: At. Spectrosc. 41 (1–2) (1986) 183.
- [22] F. Tuomisto, I. Makkonen, Rev. Mod. Phys. 85 (2013) 1583.
- [23] R. Krause-Rehberg, H.S. Leipner, Positron Annihilation in Semiconductors, Defect Studies, in: Springer Series in Solid-State Sciences, vol. 127, Springer, Berlin, 1999.
- [24] J. Toivonen, T. Hakkarainen, M. Sopanen, H. Lipsanen, J. Oila, K. Saarinen, Appl. Phys. Lett. 82 (2003).
- [25] K. Santhakumar, K.G.M. Nair, R. Kesavamoorthy, V. Ravichandran, Nucl. Instrum. Methods Phys. Res. B 212 (2003) 381.
- [26] M. Katsikini, K. Papagelis, E.C. Paloura, S. Ves, J. Appl. Phys. 94 (2003) 4389.
- [27] A. van Veen, H. Schut, J. de Vries, R.A. Hakvoort, M.R. Ijpm, AIP Conf. Proc. 218 (1991) 171.
- [28] G. Kresse, J. Furthmüller, Phys. Rev. B 54 (1996) 11169.
- [29] J.P. Perdew, K. Burke, M. Ernzerhof, Phys. Rev. Lett. 77 (1996) 3865.
- [30] P. Dev, Y. Xue, P. Zhang, Phys. Rev. Lett. 100 (2008) 117204.
- [31] P. Dev, P. Zhang, Phys. Rev. B 81 (2010) 085207.
- [32] A.C. Durst, R.N. Bhatt, P.A. Wolff, Phys. Rev. B 65 (2001) 235205.
- [33] R.N. Bhatt, M. Berciu, M.P. Kennett, X. Wan, J. Supercond. 15 (2002) 71.